REPORT DOCUMENTATION PAGE

Form Approved OMB No. 0704-0188

1. REPORT DATE *(DD-MM-YYYY)*
21-10-2010

2. REPORT TYPE
Final Report

3. DATES COVERED *(From – To)*
15 April 2009 - 15-Apr-10

4. TITLE AND SUBTITLE
SYNTHESIS AND CHARACTERIZATION OF 2 D CONJUGATED ORGANIC POLYMERS: The electrochemical approach

5a. CONTRACT NUMBER
FA8655-09-1-3019

5b. GRANT NUMBER

5c. PROGRAM ELEMENT NUMBER

6. AUTHOR(S)
Professor Steven De Feyter

5d. PROJECT NUMBER

5d. TASK NUMBER

5e. WORK UNIT NUMBER

7. PERFORMING ORGANIZATION NAME(S) AND ADDRESS(ES)
Katholieke Universiteit Leuven
Celestijnenlaan 200 F
Heverlee B-3001
Belgium

8. PERFORMING ORGANIZATION REPORT NUMBER
N/A

9. SPONSORING/MONITORING AGENCY NAME(S) AND ADDRESS(ES)
EOARD
Unit 4515 BOX 14
APO AE 09421

10. SPONSOR/MONITOR'S ACRONYM(S)

11. SPONSOR/MONITOR'S REPORT NUMBER(S)
Grant 09-3019

12. DISTRIBUTION/AVAILABILITY STATEMENT

Approved for public release; distribution is unlimited.

13. SUPPLEMENTARY NOTES

14. ABSTRACT

The proposed research covers the areas of organic chemistry, surface science and nanoscience. Classical polymerization of organic molecules involves two reactive sites of a monomer, yielding one–dimensional polymer chains. Even when multiple reactive sites are involved, the resulting polymer has a disordered 3D structure (e.g., hyperbranched polymers of dendrimers) due to conformational freedom and internal strain of the oligomeric intermediates. The need for well–ordered organic polymers for electronic applications and nanotechnology in general stimulates the search for novel approaches to polymerization. ***The goal is to develop two–dimensional conjugated organic polymers, which currently do not exist****. The bulk structure of these organic 2D polymers is expected to resemble that of graphite, with well-defined covalently assembled planar sheets separated by a π-π stacking distance (ca. 3.5 Å). Electronic conjugation, spread in two directions, and a high degree of order are expected to confer special electronic properties (low bang gap, high charge mobility, high charge storage capacity, sensing capabilities with ultralow detection limit, etc.) to these materials, which should also be very robust (as for organics). Such advanced polymeric materials will have a variety of applications of interest for the Air Force, for example in the development of novel aircraft and rocket components.*

15. SUBJECT TERMS
EOARD, Polymer Chemistry, organic polymers, 2-D polymers

16. SECURITY CLASSIFICATION OF:			17. LIMITATION OF ABSTRACT	18, NUMBER OF PAGES	19a. NAME OF RESPONSIBLE PERSON
a. REPORT	**b. ABSTRACT**	**c. THIS PAGE**			WYNN SANDERS, Maj, USAF
UNCLAS	UNCLAS	UNCLAS	UL	16	**19b. TELEPHONE NUMBER** *(Include area code)* +44 (0)1895 616 007

Standard Form 298 (Rev. 8/98)
Prescribed by ANSI Std. Z39-18

Grant, 093019, entitled "SYNTHESIS AND CHARACTERIZATION OF 2 D CONJUGATED ORGANIC POLYMERS: The electrochemical approach"

Final report

Steven De Feyter, Yonghai Song
Katholieke Universiteit Leuven
Department of Chemistry
Celestijnenlaan 200 F
B-3001 Leuven
Belgium

A. INTRODUCTION/ABSTRACT:

The proposed research covers the areas of organic chemistry, surface science and nanoscience. Classical polymerization of organic molecules involves two reactive sites of a monomer, yielding one–dimensional polymer chains. Even when multiple reactive sites are involved, the resulting polymer has a disordered 3D structure (e.g., hyperbranched polymers of dendrimers) due to conformational freedom and internal strain of the oligomeric intermediates. The need for well–ordered organic polymers for electronic applications and nanotechnology in general stimulates the search for novel approaches to polymerization. ***The goal is to develop two–dimensional conjugated organic polymers, which currently do not exist****. The bulk structure of these organic 2D polymers is expected to resemble that of graphite, with well-defined covalently assembled planar sheets separated by a π-π stacking distance (ca. 3.5 Å). Electronic conjugation, spread in two directions, and a high degree of order are expected to confer special electronic properties (low bang gap, high charge mobility, high charge storage capacity, sensing capabilities with ultralow detection limit, etc.) to these materials, which should also be very robust (as for organics). Such advanced polymeric materials will have a variety of applications of interest for the Air Force, for example in the development of novel aircraft and rocket components.*

B. TECHNICAL PROPOSAL/DESCRIPTION OF WORK:

This research project was motivated by contacts with Dr. Dmitrii F. Perepichka (McGill Unversity) and Dr. Federico Rosei (INRS–EMT, Univ. of Quebec) who some time ago started a challenging and potentially high impact interdisciplinary research project "*The synthesis and characterization of 2D conjugated organic polymers*". They have developed heterocyclic multidentate monomers specifically designed for this purpose by Density Functional Theory calculations. The design should eliminate any steric hindrances in the oligomers which would result in non-planar conformations. Dmitrii F. Perepichka has already synthesized suitable monomers to serve as building blocks for 2D conjugated polymers. Several promising functional monomers have been realized.

The elaboration of suitable polymerization conditions and characterization of the obtained polymer structures requires a synergistic effort between an organic chemist and surface scientists.

The focus is the formation of individual sheets of a 2D polymer, and their characterization mainly by means of scanning probe microscopy. The role of the Leuven partner is the use of electrochemical scanning tunneling microscopy to achieve these goals. The Leuven group will focus on:

Electrochemical oxidative polymerization: Electrochemical oxidative polymerization is widely used to prepare conducting organic films, particularly for insoluble conjugated polymers. Recently Sakaguchi et al. have demonstrated that highly ordered 1D polythiophene strands can be prepared as a submonolayer on a gold surface by pulsed electrochemical deposition.[1] We will apply this method to induce the formation of 2D conjugated nanostructures of monomers in solution. Establishing the right conditions (potential pulse width and height, electrolyte, surface), we expect to confine the polymerization to the absorbed molecules (due to preferential electron transfer), so that the formation of large planar sheets on the surface will dominate the growth of disordered oligomers in solution. The deposition of 1D polythiophene strands follow the threefold motif of the Au(111) surface. Thus, this surface is most suitable for the tridentate monomers. We note that despite of preliminary success by Sakaguchi,[1] there is little understanding of the mechanism of such epitaxial growth. This understanding is critical for expanding the approach to 2D polymers. Using in-situ electrochemical STM on Au(111), the Leuven group plans to investigate the early stages of polymerization, in order to pinpoint the critical stages of the process.

1,4-Addition polymerization: 1,4-Addition polymerization was discovered in late 1960s as a solid state reaction transforming substituted diacetylenes into conjugated 1D polymers.[2,3] It is sensitive to crystal packing and usually proceeds with the preservation of crystallinity. Polymerization of diacetylene derivatives in a self-assembled monolayer on HOPG has been studied by Scanning Tunneling Microscopy since late 1990s independently by De Feyter et al.[4,5] and Aono et al.[6,7,8] The reaction yielded 1D conjugated "wires" bound by van-der-Waals or hydrogen-bonded interactions in two dimensions. Furthermore, De Feyter et al.[5] reported the formation of a covalent 2D poly(diacetylene) by surface polymerization of monomers containing two polymerizable groups. However, the planarity of the formed structure was provided only by the surface (otherwise the conformational freedom of non-conjugated alkyl chains would result in folding the polymer in a disordered 3D object). More importantly, electronically this polymer is still one-dimensional as the conjugation is confined within each poly(diacetylene) line. To obtain a 2D conjugated poly(diacetylene), we will use a fully conjugated bi-functional monomer, which can self-assemble in monolayers, allowing for a topochemical polymerization. The new monomer has been specifically designed for such purpose. Once the optimally structured monolayer is prepared on a surface it can be polymerized by either: photoinitiation or STM-tip voltage pulse initiation (allowing selective polymerization of the chosen region and a fine control of the polymer' size)

In this **collaborative** effort, the specific task of the Leuven group is to investigate the electro-oxidative polymerisation of the relevant compounds at the interface between metallic substrates and aqueous electrolyte in order to make two-dimensional conjugated polymers. As successfully demonstrated by the applicant, lack of solubility in water does not impede the formation of highly ordered patterns on metallic substrates.[9,10] This approach holds great promise for the successful realization of the objectives.

In conclusion, the goal of the proposal is to demonstrate the feasibility of the concept of 2D conjugated polymers by surface confined polymerization in monolayers, carried out by electro-oxidative reactions under potential control and probed by electrochemical scanning tunneling microscopy.

References

1 Sakaguchi, H.; Matsumura, H.; Gong, H. *Nat. Mater.* **2004**, *3*, 551.
2 Wegner, G. *Z. Naturforsch,* **1969**, *24b*, 824.
3 Ogawa, T. *Prog. Polym Sci.* **1995**, *20*, 943.

4 Grim, P.C.M, De Feyter, S., Gesquiere, A., Vanoppen, P., Rucker, M., Valiyaveettil, S., Moessner, G., Mullen, K., De Schryver, F.C., *Angew. Chem. Int. Ed.* **1997**, 36, 23, 2601
5 Miura, A.; De Feyter, S.; Abdel-Mottaleb, M.M.S.; Gesquière, A.; Grim, P.C.M.; Moessner, G.; Sieffert, M.; Klapper, M.; Müllen, K.; De Schryver, F.C. *Langmuir* **2003**, *19*, 6474.
6 Takami, T.; Ozaki, H.; Kasuga, M.; et al. *Angew. Chem. Int. Ed.* **1997**, *36*, 2755.
7 Okawa, Y.; Aono, M. *Nature* **2001**, *409*, 683.
8 Okawa, Y.; Aono, M. *Surf. Sci.* **2002**, *19*, 187.
9 Klymchenko, A.S.; Furukawa, S.; Mullen, K.; Van der Auweraer, M.; De Feyter, S, *Nano Letters* **2007**, *3*, 791.
10. Klymchenko, A.S.; Furukawa, S.; Mullen, K.; Van der Auweraer, M.; De Feyter, S, *Nano Letters* **2008**, *8*, 1163.
11 Yang, J.-S.; Swager, T. M. *J. Am. Chem. Soc.* **1998**, *120*, 11864.
12 Ho, H.A.; Bera-Aberem, M.; Leclerc, M. *Chem. Eur. J.* **2005**, *11*, 1718.
13 Ong, B. S.; Wu, Y.; Liu, P.; Gardner, S. *J. Am. Chem. Soc.* **2004**, *126*, 3378.

Realisations

Dr. Yonghai Song, an expert in electrochemistry, was hired to work on this project. He officially started to work on the project on April 16, 2009. He was already in the Leuven team since beginning of 2009. Most of the research activities involved scanning probe microscopy experiments, and in particular scanning tunneling microscopy experiments under electrochemical control. The substrate of choice was gold, namely Au(111). Prior to investigating the self-assembly of promising compounds under electrochemical conditions, the self-assembly of these water-insoluble compounds were investigated at the air/gold interface.

The compounds were provided by Prof. Dmitrii F. Perepichka from McGill University.

Prior to the start of the project, Steven De Feyter, the scientist in charge has spent a week (January 2009) in the research groups of Dmitrii F. Perepichka and Federico Rosei to discuss the collaboration. In August 2009, Prof. Perepichka has spent about a week in the research group of the scientist in charge at the Katholieke Universiteit Leuven, in Belgium.

The compounds were designed and synthesized to have appropriate oxidation potentials for the oxidative polymerization of the compounds on the surface. Prior to the attempts to polymerize these species on the surface, their self-assembling properties were evaluated on Au(111). In addition to the self-assembling properties, a critical aspect is the stability of the substrate under the electrochemical conditions required to induce the surface reactions; though gold is 'chemically inert', the potentials needed to oxidize some of the compounds under investigation are close to the onset of the oxidation of the Au(111) substrate. Obviously, such conditions are to be avoided.

A detailed account of the results obtained with some of the systems is indicated below.

During the period of the grant, we did not succeed in the formation of highly regular two-dimensional polymers. However, some experiments indicate that the compounds investigated might react on the local scale. Regardless if the molecules reacted, most molecular systems showed a clear potential dependent response in terms of the molecular organization on the surfaces.

Self-Assembly of Tetrathienoanthracene Derivatives on Au(111) Surface Probed by Scanning Tunneling Microscopy at the air/solid interface and at electrified interfaces

Yonghai Song*, Shengbin Lei, Dmitrii F. Perepichka* and Steven De Feyter*

Laboratory of Photochemistry and Spectroscopy and INPAC-Institute for Nanoscale Physics and Chemistry, Katholieke Universiteit Leuven, Leuven, Belgium

*Coresponding author:
INPAC – Prof. Steven De Feyter
Celestijnenlaan 200F
B-3001 Leuven
Belgium
Phone: +32 (0)16 32 79 21
Fax: +32 (0)16 32 79 90
E-mail: Steven.DeFeyter@chem.kuleuven.be

Introduction

With excellent electronic properties and high stability under ambient conditions, poly- and oligothiophenes have found applications as materials for organic light-emitting diodes, thin film transistors, and photovoltaics. Controlling the arrangement of conjugated polymers at a molecular level can have important consequences on their electronic properties and device applications. This concept has stimulated many studies to look into the packing order of conjugated polymers with different molecular dimensions. Although the fabrication of practical devices involves the deposition of multilayered thin films, it is fair to state that the structure of the first monolayer can be influential to the subsequent growth of thin films. Thus, elucidating how oligothiophene molecules interact with the substrate can be important for their future applications.

A number of STM studies are devoted to polythiophene and oligothiophenes adsorbed on highly oriented pyrolytic graphite (HOPG) and molybdenum disulfide (MoS2) surfaces. Frequently, STM results show that oligomers with alkyl substituents at β-positions tend to form ordered structure on HOPG with the alkyl side chains aligned along one of the main crystallographic axes of the substrate. Regioregular polythiophenes always form self-organized polycrystals in comparable lamellar structures with 3-fold symmetry on HOPG surface both at the liquid-solid interface and in dry films. In contrast, R,R_0- and R-substituted derivatives are adsorbed preferably on MoS_2 rather than on HOPG. In addition, STM provides information about intermolecular and interfacial interactions, which are important from the viewpoint of applying these materials in thin-film devices. Another strength of STM technique lies in its capability to reveal local surface events, such as the transformation of ordered phases and mobility of defects.

Experimnetal Section

Tetrathienoanthracene derivatives (3TTA and 2TTA) have been effectively synthesized as previously reported and their chemical structures are shown in Chart 1. Chloroform (Spectroscopy grade) was purchased from Kanto Chemical Co. The aqueous electrolyte solution was prepared with $HClO_4$ (Cica-Merck) and ultrapure water (Milli-Q SP-TOC; 18.2MΩ cm). All electrolyte solutions were purged with argon gas before use. A gold(111) single crystal was purchased from MaTeck (Julich, Germany).

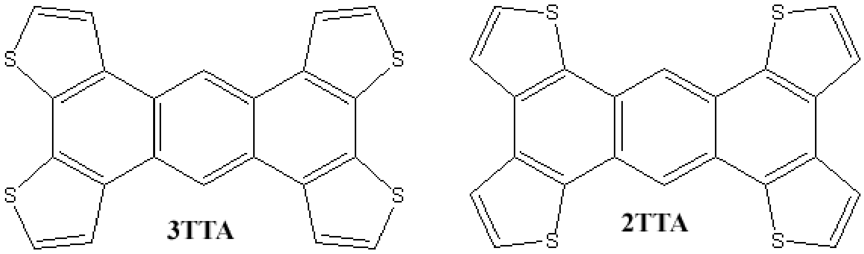

Chart 1. Chemical structure of Tetrathienoanthracene derivatives: 3TTA (left) and 2TTA (right).

Prior to each experiment a clean gold(111) surface was prepared as followed. The gold(111) surface was immersed into 0.1 M H_2SO_4 solution and subsequently an anodic potential of 10 V was applied between the gold(111) electrode and a platinum foil for about 60 s. Then the crystal was rinsed with Milli-Q water. To remove off the oxidized gold on the surface, the crystal was immersed into 0.1 M HCl for 3 min. After the crystal was rinsed with Milli-Q water, the gold(111) was flame-annealed with a butane torch and cooled in an argon atmosphere. The tetrathienoanthracenes derivatives were dissolved first in chloroform and then a drop of the mixture was dropped on the freshly prepared gold(111) surface. After 30 s, the sample was rinsed with chloroform to remove off the excess of molecules and mounted into the electrochemical cell. The cell was filled with 0.1 M $HClO_4$ electrolyte and the crystal was kept under potential control.

All electrochemical scanning tunneling microscope (ECSTM) experiments have been performed using a home-built instrument. A platinum wire was used as a pseudo reference electrode. All potentials were calibrated and are rescaled to the reversible hydrogen electrode (RHE). The whole ECSTM was housed in a sealed aluminum chamber with electrical and liquid feed through and filled with oxygen-free argon. The ECSTM tips were electrochemically etched from a 0.25 mm tungsten wire in 2 M KOH solution and subsequently isolated by passing the tip through a drop of hot-glue. All the ECSTM measurements were performed in 0.1 M $HClO_4$ as supporting electrolyte, which was deoxygenated with argon gas several hours before use. Ex-situ STM experiments were performed using a Nanoscope IIId (Digital Instruments) along with an external pulse/function generator (model HP 8111 A). Pt/Ir wire (80%/20%, diameter 0.2 mm) was mechanically cut and used as tips for ex-situ STM measurement.

Results and Discussion

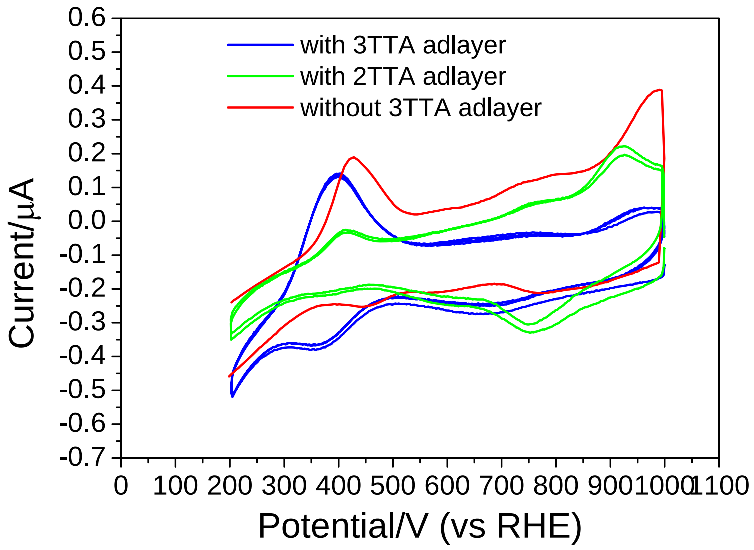

Figure 1. Typical cyclic voltammograms (CVs) of bare Au(111) (red curve), 3TTA-covered Au(111) (blue curve) and 2TTA-covered Au(111) (green curve) electrodes in 0.10 M $HClO_4$. The scan rate was 10 mV s^{-1}.

Voltammetry. Figure 1 shows typical cyclic voltammograms (CVs) recorded at a scan rate of 10 mV s^{-1} with well-defined Au(111) electrodes with and without 3TTA adlayers in 0.10 M $HClO_4$. The CV for bare Au(111) is characteristically similar as those of clean surfaces reported by others (red curve). The 3TTA and 2TTA adsorption results in the decrease of double-layer charging current of Au(111) electrode, suggesting the Au(111) electrode is covered by TMA molecules (blue curve and green curve).

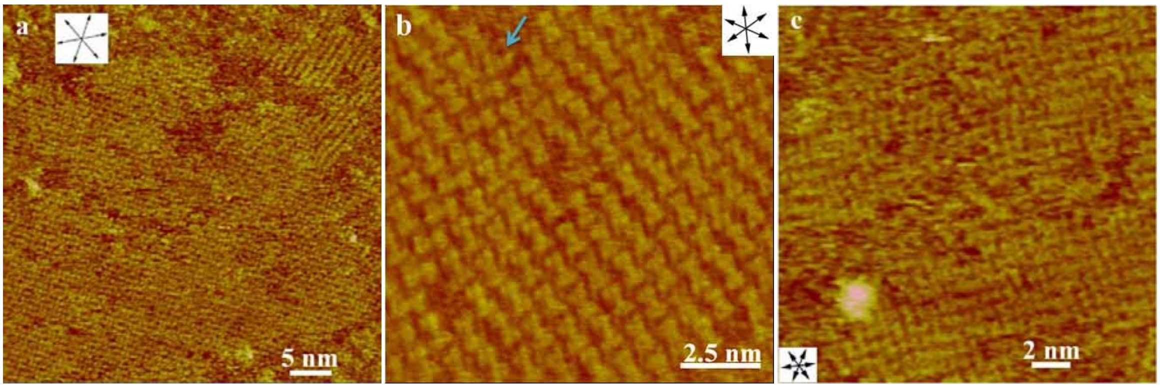

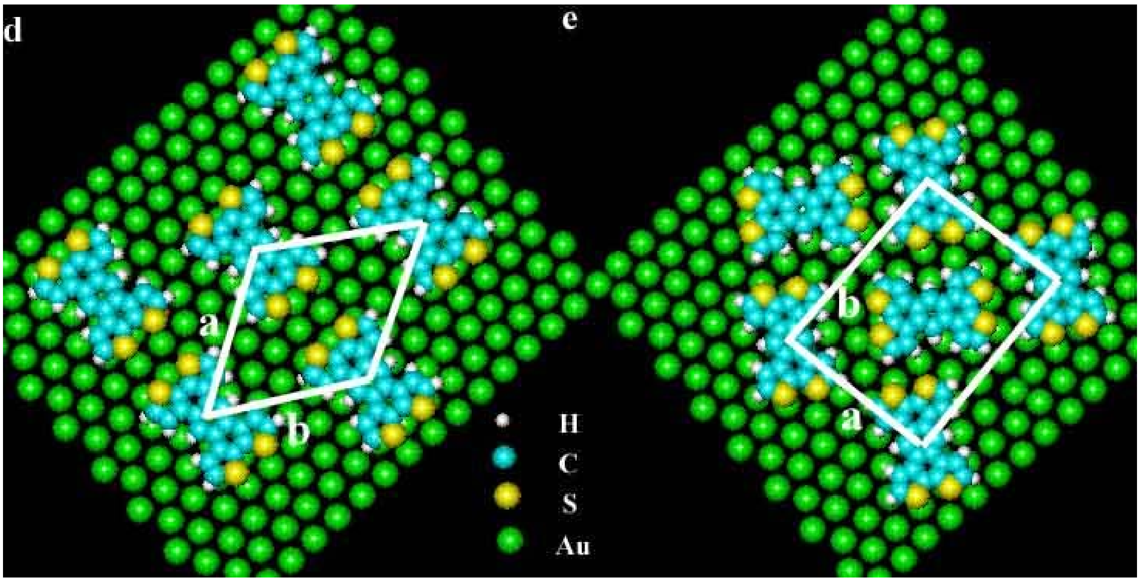

Figure 2 Large scale (a) and high-resolution (b $(3\sqrt{3}\times 3\sqrt{3})\mathrm{R}30^{\circ}$, c $(7\times 3\sqrt{3})$rect) STM images of 3-TTA adlayer on Au(111) surface acquired in air. Proposed model and unit cell of 3-TTA adlayer on the Au(111) surface (d, e). The bias voltage and the tunneling current were 0.85 V and 500 pA, respectively. The set of three arrows indicated the close-packed directions of the Au(111) substrate.

Figure 2a shows a 46 x 46 nm^2 STM topographic scan of a 3TTA-coated Au(111) electrode obtained in air. The imaging parameters, such as feedback current and bias voltage, are typically 0.5 nA and 0.85 V, respectively. The ordered arrangement of 3TTA molecules is apparent, where the domain size ranges from several tens to several hundreds of nanometers. Each domain consists of alternating bright and dark stripes running parallel to the <121> directions of the Au(111) substrate. The patchy appearance of the electrode surface was derived from the presence of multiple rotational domains. Two neighboring domains are rotated by 60º or 120 º with respect to each other. The arrangement of 3TTA admolecules of different domains in Figure 2a were all observed and compared (data were not shown here), and all molecules in these three domains were arranged similarly. The herringbone features of a reconstructed Au(111) was not found at all, suggesting the reconstructed Au(111)-(22 x √3) is lifted to a (1 x 1) surface.

A high-resolution STM image is shown in Figure 2b as a representative to reveal the details of the internal molecular structure of the 3TTA adlattice. The image reveals that the 3TTA molecules in one lamella are arranged in head-to-tail from. Such an arrangement could enhance intermolecular S-S interaction and subsequently stabilize the molecular adlayer. The backbones of 3TTA admolecules are all aligned along the <121> direction of Au(111). The average separation between 3TTA molecules as measured on STM images is ~1.45 nm, which means that the 3TTA molecule fits well with the lattice structure of the Au(111) surface. These results and the molecular model are in line with those previously reported for π-conjugated systems, which show that these organic functionalities are imaged as protrusions by the STM. The unit cell of the ordered structure is represented by the parallelogram drawn in Figure 2d, where the two unit vectors a and b, measured to be 1.45±0.05 and 1.45±0.05 nm, are aligned along the <121> and <121> directions, respectively. These values correspond to 3√3 and 3√3 times of the Au lattice parameter (i.e., 3√3 x 0.289 and 3√3 x 0.289 nm), which indicates a (3√3 x 3√3)R30º structure with one molecule per unit cell. A proposed model of a 3TTA adlayer on the Au(111) surface is presented in Figure 2d. The surface concentration is measured to be 7.58 x 10^{-11} mol cm^{-2}.

Accidentally, several domains with different details of the internal molecular structure of the 3TTA adlattice from above discussion were found as shown in Figure 2c. The image reveals that the 3TTA molecules in one lamella are parallel to each other, while the neighboring lamellae are rotated by 90º. The backbones of 3TTA admolecules in one lamella are aligned along the <121> direction of Au(111) and in another lamella are aligned along the <110> direction of Au(111). The unit cell of the ordered structure is represented by the rectangle drawn in Figure 2e, where the two unit cell vectors a and b, measured to be 1.45±0.05 and 2.0±0.05 nm, are aligned along the <121> and <110> directions, respectively. These values correspond to 7 and 3√3 times the Au lattice parameter (i.e., 7 x 0.289 and 3√3 x 0.289 nm), which indicates a (7 x 3√3)rect structure with two molecules per unit cell. A proposed model of a 3TTA adlayer on the Au(111) surface is presented in Figure 2e. The surface concentration should be 1.13 x 10^{-10} mol cm^{-2}, which is a bit higher than observed for the previous structure.

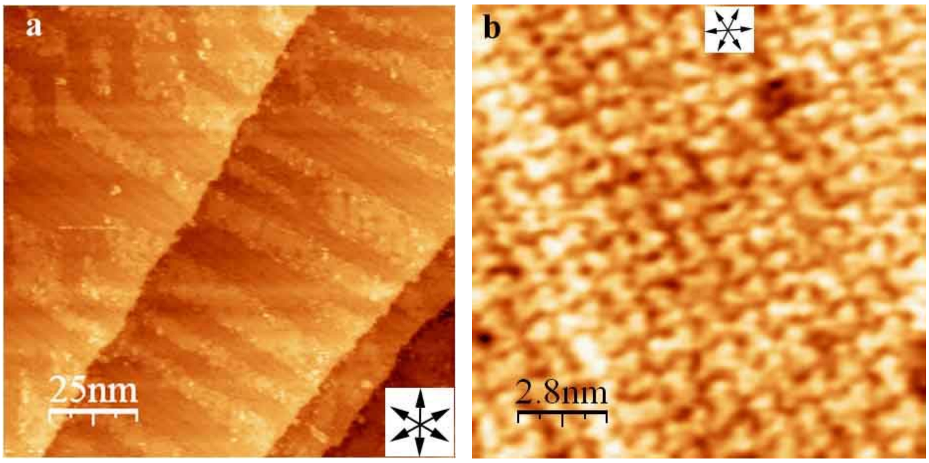

Figure 3. Large scale (a) and high-resolution (b) STM images of 3TTA adlayer on Au(111) acquired in 0.10 M $HClO_4$ at E = 0.20 V (vs RHE). The bias voltage and the tunneling current were -22 mV and 100 pA, respectively. The set of three arrows indicated the close-packed directions.

Figure 3a shows a 125 x 125 nm^2 EC-STM topographic scan of a 3TTA-coated Au(111) electrode obtained in 0.10 M $HClO_4$ at 0.2 V. The herringbone features of the reconstructed Au(111)-(22 x √3) is apparent. Judged by the density of the herringbone features, the reconstructed Au(111)-(22 x √3) is not partly lifted to a (1 x 1) surface. A high-resolution STM image is shown in Figure 3b as a representative to reveal the details of the internal molecular structure of the 3TTA adlattice, which is the same as the previous second structure observed by STM in air.

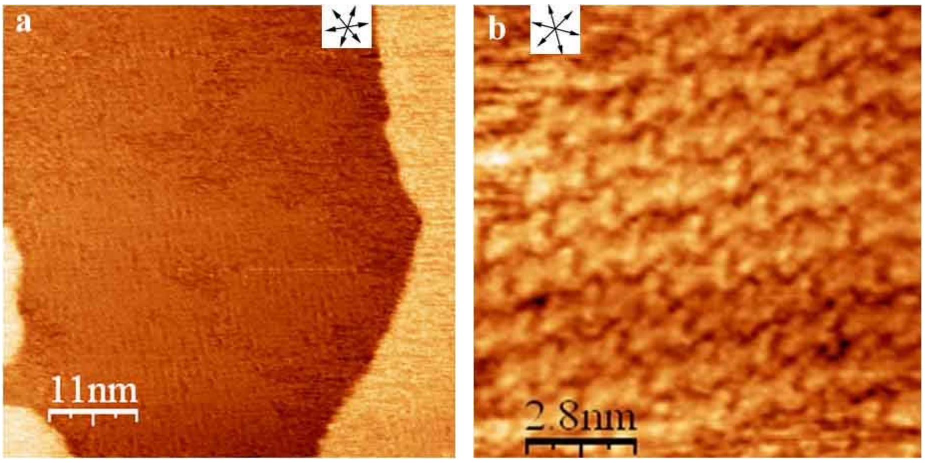

Figure 4. Large scale (a) and high-resolution (b) STM images of 3TTA adlayer on Au(111) acquired in 0.10 M $HClO_4$ at E = 0.60 V (vs RHE). The bias voltage and the tunneling current were 150 mV and 100 pA, respectively. The set of three arrows indicated the close-packed directions.

When the working potential is controlled to be 0.6 V, the large-scale EC-STM topographic scan of a 3TTA-coated Au(111) electrode obtained in 0.10 M $HClO_4$ at 0.2 V reveals many lamella as shown in Figure 4a. Close inspection of these lamellas discloses that they are the same as the previous first structure. However, the herringbone features of the reconstructed Au(111)-(22 x √3) is not found, suggesting the reconstructed Au(111)-(22 x √3) is lifted to a (1 x 1) surface. A high-resolution STM image is shown in Figure 4b as a representative to reveal the details of the internal molecular structure of the 3TTA adlattice, which is the same as the previous first structure observed by STM in air.

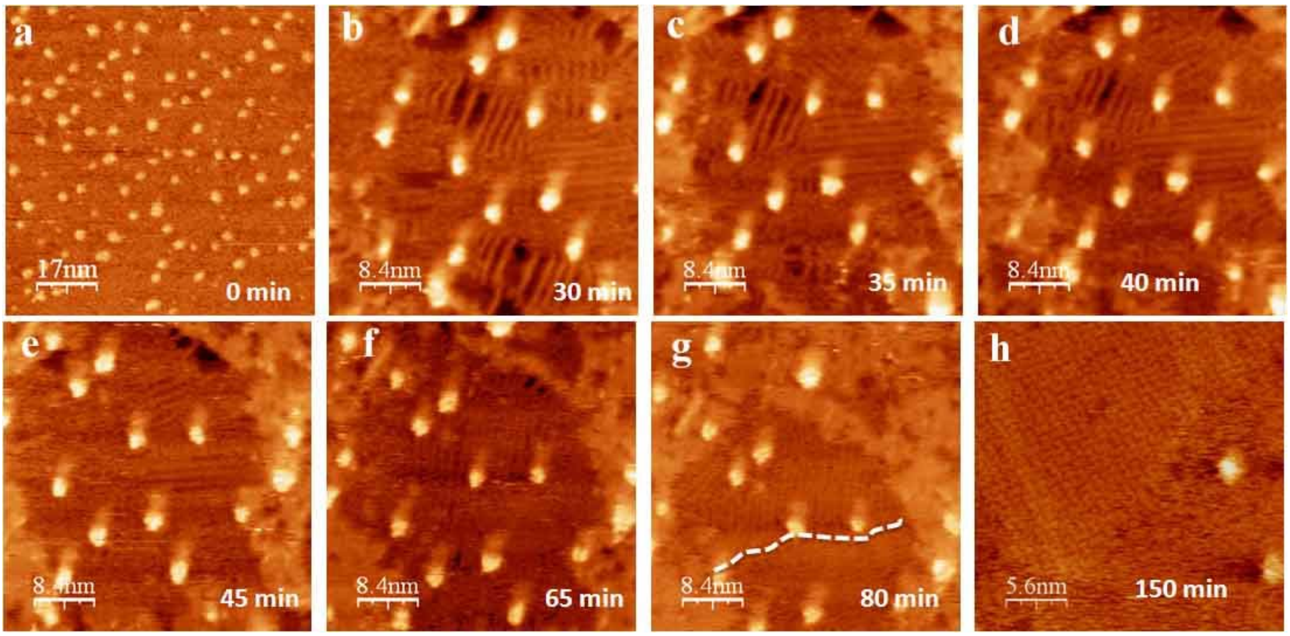

Figure 5. Time-dependent STM images depicting dynamic changes occurring at a monolayer of 3TTA on Au(111) acquired at E=0.20 V (vs RHE) in 0.10 M $HClO_4$.

Figure 5 presents a series of time-dependent EC-STM images of 3TTA adlayers on Au(111) in 0.10 M $HClO_4$ with an electrode potential held at E=0.20 V after 3TTA-coated Au(111) electrode is scanned in the potential range from 0 V to +1.1 V for 3 cycles. As can be seen in Figure 5a, the initial stage of STM imaging revealed a unreconstructed Au(111)-(1 x 1) surface, characterized by some gold clusters as shown in Figure 5a. Interestingly, the growth of the two-dimensional (2D) structures appears, indicative of 3TTA adsorption on the Au(111) surface after 30 min (Figure 5b). In the STM image, every bright line can be attributed to one lamella of well-ordered molecules. As the time increases (Figure 5c, d, e and f), some structures gradually underwent rearrangement with crystal growth and packing arrangement becoming more homogeneous. Finally, the more stable and homogeneous 3TTA structures were obtained on Au(111) electrode at this potential after 80 min from the onset of STM imaging (Figure 5g). High-resolution ECSTM image indicates that internal molecular structure of the 3TTA adlattice is the same as the previous second structure. It is to be noted that all these STM images were acquired in the same area as indicated by the large bright feature at these images to reliably investigate the local surface events that transpired.

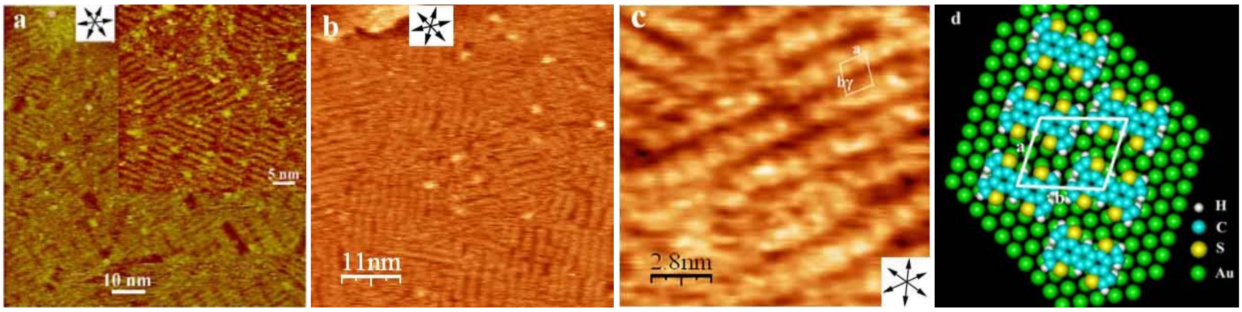

Figure 6. Large-scale (a, b) and high-resolution (c) STM images of 2TTA adlayer on Au(111) surface acquired in air (a) and in 0.10 M $HClO_4$ at E = 0.20 V (vs RHE) (b, c). The bias voltage and the tunneling current were 0.75 V and 200 pA for image (a) and 0.25 V and 100 pA for image (b, c), respectively. The set of three arrows indicated the close-packed directions.

Figure 6a and b shows large-scale STM topographic scans of 2TTA-coated Au(111) electrodes obtained in air and in 0.10 M $HClO_4$ at 0.2 V, respectively. The results clearly indicate that the 2TTA adlattice is the same as that of in 0.10 M $HClO_4$ at 0.2 V. The ordered arrangement of 2TTA molecules is apparent, while the domain is very small. Each domain consists of alternating bright and dark stripes running parallel to the <110> directions of the Au(111) substrate. Two neighboring domains are rotated by 60º or 120 º with respect to each other. The corrugated pairwise lines are herringbone features of a reconstructed Au(111). A high-resolution STM image is shown in Figure 6c as a representative to reveal the details of the internal molecular structure of the 2TTA adlattice. The image reveals that the 2TTA molecules in one lamella are arranged side-by-side. Such an arrangement could enhance intermolecular S-S interaction and subsequently stabilize the molecular adlayer. The backbones of 2TTA admolecules are all aligned along the <011> direction of Au(111). The average separation between 2TTA molecules along lamella as measured on STM images is ~1.2 nm. The unit cell of the ordered structure is represented by the parallelogram drawn in Figure 6c with one molecule per unit cell, where the two unit vectors a and b are measured to be 1.2±0.05 and 1.7±0.05 nm. A proposed model of a 2TTA adlayer on the Au(111) surface is presented in Figure 6d.

Conclusion

Two kinds of 3TTA adlattice on Au(111) surface is found by STM in air. High-resolution STM images reveal the 3TTA molecules in one lamella are arranged in heat-to-tail from in one adlattice, where the 3TTA molecules adsorb on Au(111)-(1x1) surface. In another adlattice that can be accidentally found, the 3TTA molecules in one lamella are parallel to each other, while the neighboring lamella are rotated by 90º. In 0.1 M $HClO_4$ at 0.2 V, 3TTA adlattice observed by ECSTM is the same as the second adlattice observed in air, where the 3TTA molecules obviously adsorb on reconstructed Au(111) surface. When the working potential is controlled to be 0.6 V, 3TTA adlattice is the same as the first adlattice observed in air. 2TTA molecules in one lamella are arranged in side-by-side from and only one adlattice is found. Such an arrangement could enhance intermolecular S-S interaction and subsequently stabilize the molecular adlayer.

Self-Assembly and Electropolymerization of TEDOT-TTB on Au(111) Probed by Electrochemical Scanning Tunneling Microscopy

Yonghai Song, Shengbin Lei, Dmitrii F. Perepichka* and Steven De Feyter*

Laboratory of Photochemistry and Spectroscopy and INPAC-Institute for Nanoscale Physics and Chemistry,
Katholieke Universiteit Leuven, Leuven, Belgium

*Coresponding author:
INPAC – Prof. Steven De Feyter
Celestijnenlaan 200F
B-3001 Leuven
Belgium
Phone: +32 (0)16 32 79 21
Fax: +32 (0)16 32 79 90
E-mail: Steven.DeFeyter@chem.kuleuven.be

Introduction

With excellent electronic properties and high stability under ambient conditions, poly- and oligo-thiophenes have found applications as materials for organic light-emitting diodes, thin film transistors, and photovoltaics. Controlling the arrangement of conjugated polymers at a molecular level can have important consequences on their electronic properties and device applications. This concept has stimulated many studies to look into the packing order of conjugated polymers with different molecular dimensions. Although the fabrication of practical devices involves the deposition of multilayered thin films, it is fair to state that the structure of the first monolayer can be influential to the subsequent growth of thin films. Thus, elucidating how oligothiophene molecules interact with the substrate can be important for their future applications.

Experimental Section

Tri-EDOT-Terthienobenzene (TEDOT-TTB) has been effectively synthesized as previously reported and the chemical structures is shown in Chart 1. Chloroform (Spectroscopy grade) was purchased from Kanto Chemical Co. The aqueous electrolyte solution was prepared with $HClO_4$ (Cica-Merck) and ultrapure water (Milli-Q SP-TOC; 18.2MΩ cm). All electrolyte solutions were purged with argon gas before use. A gold(111) single crystal was purchased from MaTeck (Julich, Germany).

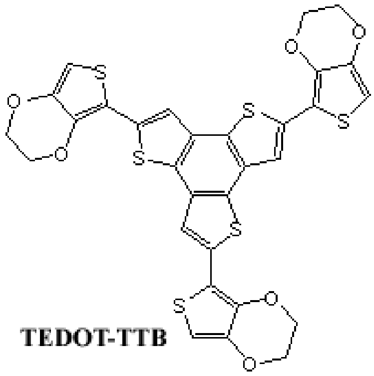

Chart 1. Chemical structure of TEDOT-TTB.

Prior to each experiment a clean gold(111) surface was prepared as follows. The gold(111) surface was immersed into 0.1 M H_2SO_4 solution and subsequently an anodic potential of 10 V was applied between the gold(111) electrode and a platinum foil for about 60 s. Then the crystal was rinsed with Milli-Q water. To remove off the oxidized gold on the surface, the crystal was immersed into 0.1 M HCl for 3 min. After the crystal was rinsed with Milli-Q water, the gold(111) was flame-annealed with a butane torch and cooled in an argon atmosphere. The TEDOT-TTB were dissolved first in chloroform and then a drop of the mixture was dropped on the freshly prepared gold(111) surface. After drying, the sample was mounted into the electrochemical cell. The cell was filled with 0.1 M $HClO_4$ electrolyte and the crystal was kept under potential control.

All electrochemical scanning tunneling microscope (EC-STM) experiments have been performed using a home-built instrument. A platinum wire was used as a pseudo reference electrode. All potentials were calibrated and are rescaled to the reversible hydrogen electrode (RHE). The whole ECSTM was housed in a sealed aluminum chamber with electrical and liquid feed through and filled with oxygen-free argon. The EC-STM tips were electrochemically etched from a 0.25 mm tungsten wire in 2 M KOH solution and subsequently isolated by passing the tip through a drop of hot-glue. All the EC-STM measurements were performed in 0.1 M $HClO_4$ as supporting electrolyte, which was deoxygenated with argon gas several hours before use.

Results and Discussion

Voltammetry. Figure 1 shows typical cyclic voltammograms (CVs) recorded at a scan rate of 10 mV s^{-1} with well-defined Au(111) electrodes with TEDOT-TTB adlayers in 0.10 M $HClO_4$. The TEDOT-TTB-modified Au(111) electrode resulted in a featureless i-V profile between 0.20 and 0.80 V, but opening the potential window to 1.2 V yielded three oxidation peaks at 0.90 V, 0.97 V and 1.07 V, respectively. These peaks were ascribed to the generation of radical cations of TEDOT-TTB molecules. This oxidation reaction appears to be irreversible as evidenced by the absence of a reduction peak in the negative scan, suggesting that the radical cations of TEDOT-TTB molecules polymerized into polyTEDOT-TTB. These oxidation peaks obviously decreased or disappeared in sequent scan. As the TEDOT-TTB molecules adsorbed on Au(111) electrode increased, these oxidization peaks obviously increased as shown Figure 1b. It is noticeable that when the TEDOT-TTB concentration increased to 100 μM, a reduction peak appeared at 0.31 V in the negative scan as shown by green curve in Figure 1b. The corresponding oxidation peak appeared at 0.43 V in the second scan. The redox peaks increased as the scan and the TEDOT-TTB concentration increased as shown by insert in Figure 1b, suggesting that they resulted from the redox of polyTEDOT-TTB. When the potential window was increased to 1.7 V, two other oxidation peaks appeared as shown in Figure 1c. The two oxidation peaks were ascribed to the oxidation of the Au(111) electrode and desorption of polyTEDOT-TTB as evidenced by the reduction peak in negative scan and obvious decrease in the second scan.

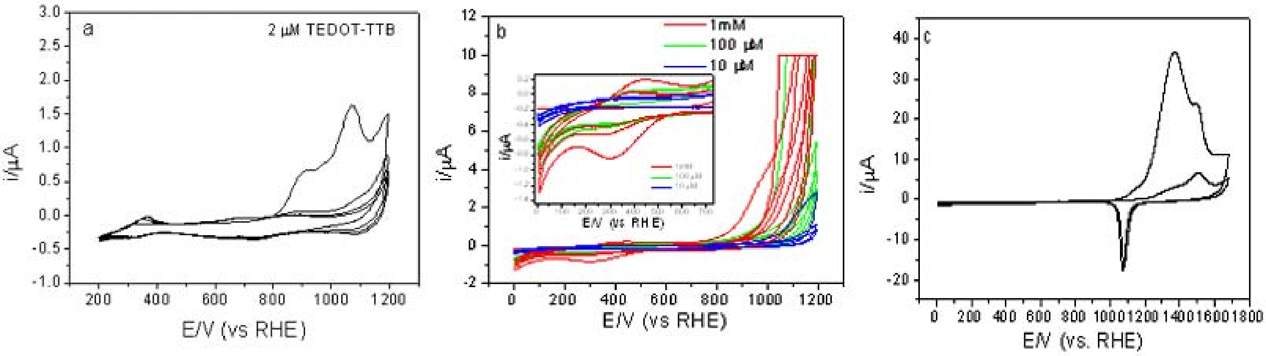

Figure 1. Typical cyclic voltammograms (CVs) of TEDOT-TTB-covered Au(111) (blue curve) and 2TTA-covered Au(111) (green curve) electrodes in 0.10 M $HClO_4$. The scan rate was 10 mV s^{-1}.

Figure 2a shows a 70 x 70 nm^2 EC-STM topographic scan of a TEDOT-TTB-coated Au(111) electrode obtained acquired in 0.10 M $HClO_4$ at E = 0.20 V (vs RHE). The imaging parameters, such as feedback current and bias voltage, are typically 100 pA and -22 mV, respectively. The ordered arrangement of TEDOT-TTB molecules is apparent. The herringbone features of a reconstructed Au(111) was not found at all, suggesting the reconstructed Au(111)-(22 x √3) is lifted to a (1 x 1) surface.

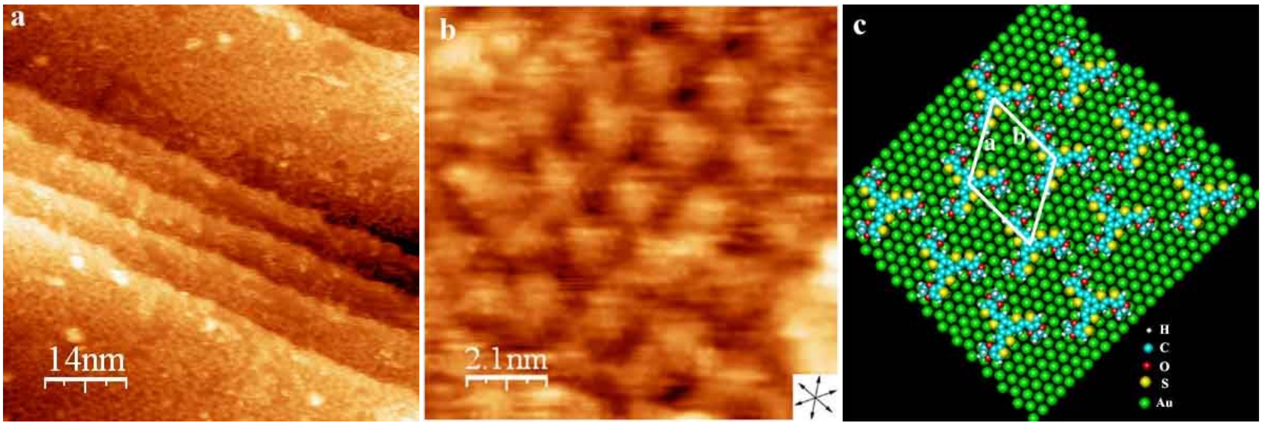

Figure 2 Large scale (a) and high-resolution (b) EC-STM images of TEDOT-TTB adlayer on Au(111) surface acquired in 0.10 M $HClO_4$ at E = 0.20 V (vs RHE). The bias voltage and the tunneling current were -22 mV and 100 pA, respectively. The set of three arrows in Figure b indicated the close-packed directions. Proposed model and unit cell of TEDOT-TTB adlayer on the Au(111) surface (c).

A high-resolution EC-STM image is shown in Figure 2b as a representative to reveal the details of the internal molecular structure of the TEDOT-TTB adlattice. The image reveals that the backbones of TEDOT-TTB admolecules are all aligned along the <121>, <112> and <211> direction of Au(111). The average separation between TEDOT-TTB molecules as measured on EC-STM images is ~2.0 nm, which means that the TEDOT-TTB molecule fits well with the lattice structure of the Au(111) surface. Such an arrangement could enhance intermolecular interaction and subsequently stabilize the molecular adlayer. These results and the molecular model are in line with those previously reported for π-conjugated systems, which show that these organic functionalities are imaged as protrusions by the EC-STM. The unit cell of the ordered structure is represented by the parallelogram drawn in Figure 2c, where the two unit vectors a and b, measured to be 2.0±0.05 and 2.0±0.06 nm, are aligned along the <121> and <112> directions, respectively. These values correspond to 4√3 and 4√3 times of the Au lattice parameter (i.e., 4√3 x 0.289 and 4√3 x 0.289

nm), which indicates a (4√3 x 4√3)R30º structure with one molecule per unit cell. A proposed model of a 3TTA adlayer on the Au(111) surface is presented in Figure 2c. The surface concentration is measured to be 4.89 x 10^{-11} mol cm^{-2}.

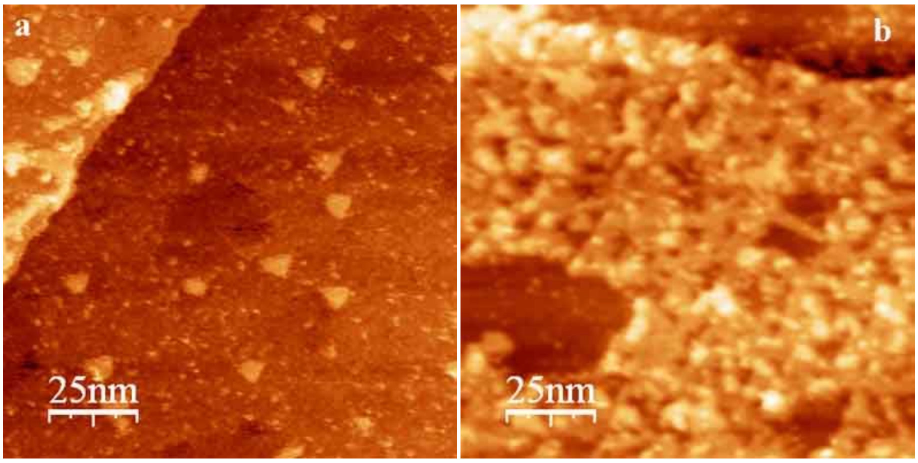

Figure 3. Large-scale EC-STM images of polyTEDOT-TTB on Au(111) acquired in 0.10 M $HClO_4$ at E = 0.20 V (vs RHE). The images were acquired after the Au(111) electrodes with TEDOT-TTB adlayer ((a) 2 µM and (b) 10 µM.) were scanned in the potential range of 0.2-1.2 V (vs RHE) in 0.10 M $HClO_4$ for 3 cycles. The bias voltage and the tunneling current were -22 mV and 100 pA, respectively.

After the Au(111) electrode with TEDOT-TTB adlayer was scanned in the potential range of 0.2-1.2 V (vs RHE) in 0.10 M $HClO_4$ for 3 cycles, some triangular sheets appeared as shown in Figure 3a. The size of the triangular sheets is uniform and estimated from the cross-section profiles (e.g., Figure 4b) is about 6-7 nm, with an “electronic height” of 0.3-0.4 nm. The triangular sheets might be ascribed to the two-dimensional polyTEDOT-TTB. When the TEDOT-TTB concentration increased to 10 µM, these two-dimensional sheets covered the whole Au(111) surface as shown in Figure 3b.

An enlarged EC-STM image of the triangular sheet from Figure 3a is shown in Figure 4a. The cross-section profile of the triangular sheet indicates that its size is about 6.8 nm and its “electronic height” is about 0.3 nm (Figure 4b), which suggests that the polyTEDOT-TTB molecule is composed of 9 TEDOT-TTB molecules. To elucidate the structure and formation mechanism of the polyTEDOT-TTB, we constructed a three-dimensional possible model of 9-polyTEDTO-TTB (Figure 4c). The TEDOT-TTB monomer is structurally optimized by energy minimization to a horizontal dimension of 1.7 nm, and a single sheet composed of 9 TEDOT-TTB monomers gives a structure with a size of 6.2 nm (Figure 4c).

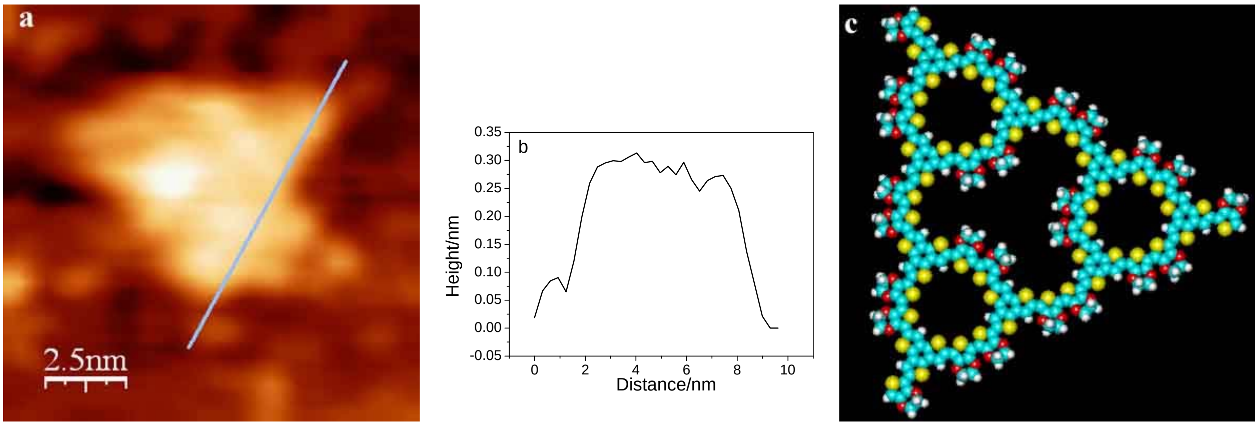

Figure 4. EC-STM images and cross-section profile of 9-polyTEDOT-TTB on Au(111) acquired in 0.10 M $HClO_4$ at E = 0.20 V (vs RHE). The bias voltage and the tunneling current were -22 mV and 100 pA, respectively. Proposed model of 9-polyTEDOT-TTB (c).

Conclusion

TEDOT-TTB formed a $(4\sqrt{3} \times 4\sqrt{3})R30^{\circ}$ adlattice with one molecule per unit cell on Au(111)-(1x1) surface. After the Au(111) electrode with TEDOT-TTB adlayer was scanned in the potential range of 0.2-1.2 V (vs RHE) in 0.10 M $HClO_4$, some triangular polyTEDOT-TTB sheets formed after the TEDOT-TTB molecules were oxidized into radical cations. The polyTEDOT-TTB sheets can potentially grow into bigger ones, eventually covering the complete surface, upon increase of the TEDOT-TTB concentration.